



Loss of Snord116 protects cardiomyocyte kinetics during ischemic stress

Lucy E. Pilcher^a, Emmaleigh Hancock^b, Akshay Neeli^a, Maria Skolnick^c,
Matthew A. Caporizzo^b, Bradley M. Palmer^b, Jeffrey L. Spees^{a,*}

^a Department of Medicine, Cardiovascular Research Institute, University of Vermont, Colchester, VT 05446, United States of America

^b Department of Molecular Physiology and Biophysics, Cardiovascular Research Institute, University of Vermont, Burlington, VT, United States of America

^c Statistical Software Support & Consulting Services, University of Vermont, Burlington, VT 05405, United States of America

ARTICLE INFO

Keywords:

Non-coding RNA

Snord116

Cardiomyocyte kinetics

Ischemic stress

ABSTRACT

Loss of Snord116, a non-coding RNA, causes Prader Willi Syndrome (PWS), a complex disorder with circadian, metabolic, neurologic, and cardiovascular phenotypes. The Snord116 paternal knockout (Snord116p⁻) mouse, a model of PWS, demonstrated differential methylation of thousands of genes involved in regulation of metabolism, epigenetics, and ion homeostasis. To determine if Snord116 expression influences the cardiomyocyte response to acute ischemia, we developed a model of ischemia and reperfusion using living myocardial slices and monitored cardiomyocyte function in slices derived from Snord116p⁻ mice and wildtype littermates (WT LM) of both sexes. We found that Snord116 loss reduced ischemia-induced systolic prolongation and delayed diastolic elongation in slices from both males and females. Furthermore, when compared with slices from males, slices from females experienced a greater increase in end-diastolic force after ischemia. We conclude that female myocardium responds more dramatically and quickly to ischemic injury in this model and that loss of Snord116 is cardioprotective; this allows for a more complete myocardial recovery following reperfusion.

1. Introduction

Cardiovascular disease is the leading cause of death worldwide, irrespective of race or sex [1]. Heart failure is a common sequela of myocardial infarction (MI), an event where vascular occlusion leads to tissue ischemia and necrosis. During ischemia, decreased ATP generation causes dysfunction of the ATP-fueled ion pumps that regulate ion homeostasis in cardiac myocytes. [2]. After MI, the ability of injured cardiac cells to recover determines the extent of damaged and necrotic tissue, which is later converted to akinetic scar tissue [3,4]. Tissue damage and negative remodeling after MI leads to progressive worsening of heart function over time and increased risk of heart failure. Thus, developing strategies and treatments to protect myocardium from the initial ischemic insult and subsequent reperfusion injury is critical to improve the prognosis for MI patients.

Albeit still under debate, some observations suggest there are important sex-based differences in patient outcomes after MI. While the female population is at lower overall risk of heart disease, females bear a higher risk for 1-year mortality after MI compared with males [5,6]. The comparatively worse early outcomes observed for female patients have been attributed, in part, to increased age for disease onset or MI in

female patients relative to males [7], but additional work is needed to determine if sex is an independent risk-factor for a worse outcome after ischemic injury. Part of the challenge of understanding sex-dependent susceptibility to ischemic injury is difficulty with monitoring myocardial structure and function in the early phase of the myocardial injury. Thus, our study specifically targets cardiac function early during ischemia and recovery and includes both male and female mice with mixed modeling to determine whether sex alone contributes to susceptibility to ischemic injury.

Non-coding RNAs have emerged as major regulators of cardiomyocyte differentiation, survival, and function [8,9]. The maternally imprinted Snord116 locus contains multiple copies of small nucleolar RNAs (snoRNAs) and a long non-coding RNA called 116hg [10]. DNA sequence deletions at the paternal Snord116 locus cause Prader-Willi Syndrome (PWS), a complex disorder characterized by sleep disturbance, mental disability, obesity, and metabolic and cardiovascular disease [11–13]. Previously, we showed Snord116 was highly-expressed in cardiac cells during running exercise, a model of physiological hypertrophy, suggesting a role for Snord116 in cardiac remodeling or myocardial stress [14]. In the murine cerebral cortex, 116hg lncRNA regulates the diurnal expression of thousands of genes by controlling

* Corresponding author.

E-mail address: jspees@uvm.edu (J.L. Spees).

<https://doi.org/10.1016/j.jmccpl.2025.100291>

Received 7 October 2024; Received in revised form 13 February 2025; Accepted 27 February 2025

Available online 2 March 2025

2772-9761/© 2025 University of Vermont.

Published by Elsevier Ltd.

This is an open access article under the CC BY-NC license

(<http://creativecommons.org/licenses/by-nc/4.0/>).

DNA methylation [9]. Coulson et al. (2018) demonstrated that 116hg regulates circadian entrained metabolic pathways and many enzymes involved in epigenetic regulation (e.g. DNA methyltransferases) [15]. Thus, we hypothesize that loss of the Snord116 locus would be detrimental during ischemia/reperfusion because altered methylation of genes involved in ion homeostasis and/or metabolism.

To investigate the effect(s) of Snord116 expression on myocardial function during ischemic stress, we developed a model of ischemia-reperfusion using living myocardial slices. Ischemia reduces the ability of cardiomyocytes to remove calcium from the sarcomere, and therefore the ability to fully relax (diastolic function). This leads to increased end diastolic force (EDF), time of contraction, and time for relaxation, and in turn reduced generated force [16,17]. Our system provides a unique opportunity to follow myocardial function through the induction and early ischemic phase, where the onset of functional changes should provide an indicator of susceptibility of the myocardium to ischemic injury. To determine if the loss of the Snord116 locus impacts cardiomyocyte function during ischemia, we generated slices from Snord116 paternal knockout (Snord116p-) mice and their wildtype littermates (WT LM). We found Snord116 deletion blunted the effect of ischemia on contractile kinetics. Furthermore, we examined the effect of sex on susceptibility to early ischemia and Snord116- protection. To our surprise, we found females exhibited increased susceptibility to contractile changes in early ischemia, to which Snord116 deletion was protective, while males were more resistant to changes in contractility in early ischemia.

2. Methods

2.1. Animals

Animal work was conducted with a protocol approved by the University of Vermont Institutional Animal Care and Use Committee (IACUC). Snord116p- mice (B6.Cg-Snord116^{tm1.1Uta}/J) were generously provided by Dr. Rudolph L. Leibel, Columbia University. Because the maternal allele is imprinted, heterozygous animals with paternal deletion of Snord116 provide a genetic background that lacks Snord116 expression (i.e., knockout mice). Snord116p- mice display multiple characteristics of Prader-Willi Syndrome (PWS) such as early-onset postnatal growth retardation, delayed sexual maturation, increased anxiety, motor learning deficit, sleep disturbance, and hyperphagia. However, they do not become obese [18].

2.2. Living myocardial slices

Animals were anesthetized by inhalation of 4 % isoflurane to effect and maintained at 2.5 % isoflurane. Animals were deeply anesthetized using isoflurane and euthanized by exsanguination upon removing the heart. Hearts were harvested from 12- to 20-week-old mice and submerged in a solution of ice cold, oxygenated modified Tyrode's solution that contained 2,3-butanedione monoxime (BDM), a contractile inhibitor. Modified Tyrode's solution: 137 mM NaCl, 4.5 mM KCl, 1.8 mM CaCl₂, 1 mM MgCl₂, 10 mM glucose, and 10 mM HEPES, at a pH between 7.3 and 7.4. Harvesting and slicing solutions contained 30 mM BDM to protect the myocardium during surgery. The right ventricle was excised and the left ventricle was cut from apex to base. Small notches were cut around the apex to allow the heart to lay flat. The heart was then glued, epicardium down, with TissueSeal™ Histoacryl surgical glue onto the plate of a vibratome (Campden Instruments) that was used to cut 200 μm thick slices. Individual slices were trimmed to the largest rectangular shape possible, while aligning the muscle fibers along the axis to be tested. 3D-printed tabs were glued onto opposing sides of the slice. The tabs were used to connect a given slice to the force gauges of an intact muscle chamber (IonOptix). Prior to establishing a baseline reading, we bathed each slice in an oxygenated Tyrode's solution that lacked BDM for at least 15 min. Slices were stimulated with 20 V at 2 Hz. Tension on

each slice was adjusted to optimize peak height. Slices were only used if they generated at least 1 mN of force. A representative example of a recorded force transient is shown in Fig. 1A.

We simulated ischemia by infusing unoxygenated glucose-free medium, until the entire bath solution was replaced (5 min). At this time, the recirculation pump was stopped for 25 min. After this period, the medium was switched back to an oxygenated solution for a recovery period of 15 min. We recorded force transients for the entire duration of the experiment (Fig. 1A) and quantified the muscle characteristics from an average of 5–20 transients, at three time points. Hereafter, the time points are referred to as: “Start”, “Ischemia”, and “Recovery” (Fig. 1A–B).

2.3. Calcein AM/Ethidium Homodimer-1 staining of slices to evaluate cell stress/death

We assayed slices from WTLM and Snord116 KO mice following the ischemia protocol. Control slices underwent continuous pacing in the same rig with perfusion for the entire duration. Control slices and those exposed to ischemia were both stained with Calcein AM for 30 mins while being paced and perfused before Ethidium Homodimer-1 (ETHD1) was added for 10 mins in relaxing solution. Both dyes were used at a concentration of 2 μM. Following the ischemia protocol, we observed similar levels of cell stress/death (i.e., ETHD1-positive cells) for slices from WTLM and Snord116 KO mice (Supplemental Fig. 6).

2.4. Work-loops

Cardiac slice force-length work loops, which mimic ventricular pressure-volume work loops, were generated by force-feedback control of slice length (IonOptix). Preload was set to isometric diastolic force and represented the target force for feedback during the refilling phase of the cardiac cycle. Afterload was set to half the developed isometric force and represented the target force during the ejection phase. Analyses included measures of end diastolic force, stroke length, and ejection fraction.

2.5. Data analysis and statistics

Various functional parameters were analyzed with a linear mixed model (SPSS software). Fixed effects included: Timepoint, Genotype, Sex, and Assay order with interaction terms Timepoint*Genotype and Timepoint*Sex. Donor mouse and slice IDs were included as random effects in the model. For selected comparisons, if the model was more accurate without including the fixed term “Tissue” (i.e., provided a lower Akaike's Information Criterion [AIC]), this fixed term was removed. For all data comparisons, *P* values ≤0.05 were considered significant. Throughout the present manuscript, number of individual slices is denoted as “*n*” and number of mice as “*N*”. Graphs were made using Origin. For all graphs, slices are represented by individual data points, boxes show SEM, and error bars show SD.

For comparisons between timepoints (Fig. 1) pairwise comparisons with Sidak's multiple comparisons were performed (all timepoints: *N* = 26, *n* = 47). For comparisons between sexes (Fig. 2) estimates of fixed effects were determined (Male: *N* = 13, *n* = 22; Female: *N* = 13, *n* = 25). Also, for comparisons between genotypes (Fig. 3) estimates of fixed effects were determined (WT LM: *N* = 14, *n* = 24; Snord116p-: *N* = 12, *n* = 23). For df/dt and work-loop analysis (Figs. 4 and 5), pairwise comparisons with Sidak's multiple comparisons were performed (Males: *N* = 12, *n* = 21; Females: *N* = 10, *n* = 21) (WT LM Male: *N* = 6, *n* = 10; WT LM Female: *N* = 6, *n* = 12; Snord116p- Male: *N* = 6, *n* = 11; Snord116p- Female: *N* = 4, *n* = 7). The linear mixed model provided a conservative analysis of the data but lacked some comparisons that we felt merited discussion. To further evaluate the data with genotype and sex separated, we performed paired, two-sided *T*-Tests between each time point (Fig. 3E, 4B and Supplemental Fig. 4) (WT LM Male: *N* = 7, *n* = 11; WT

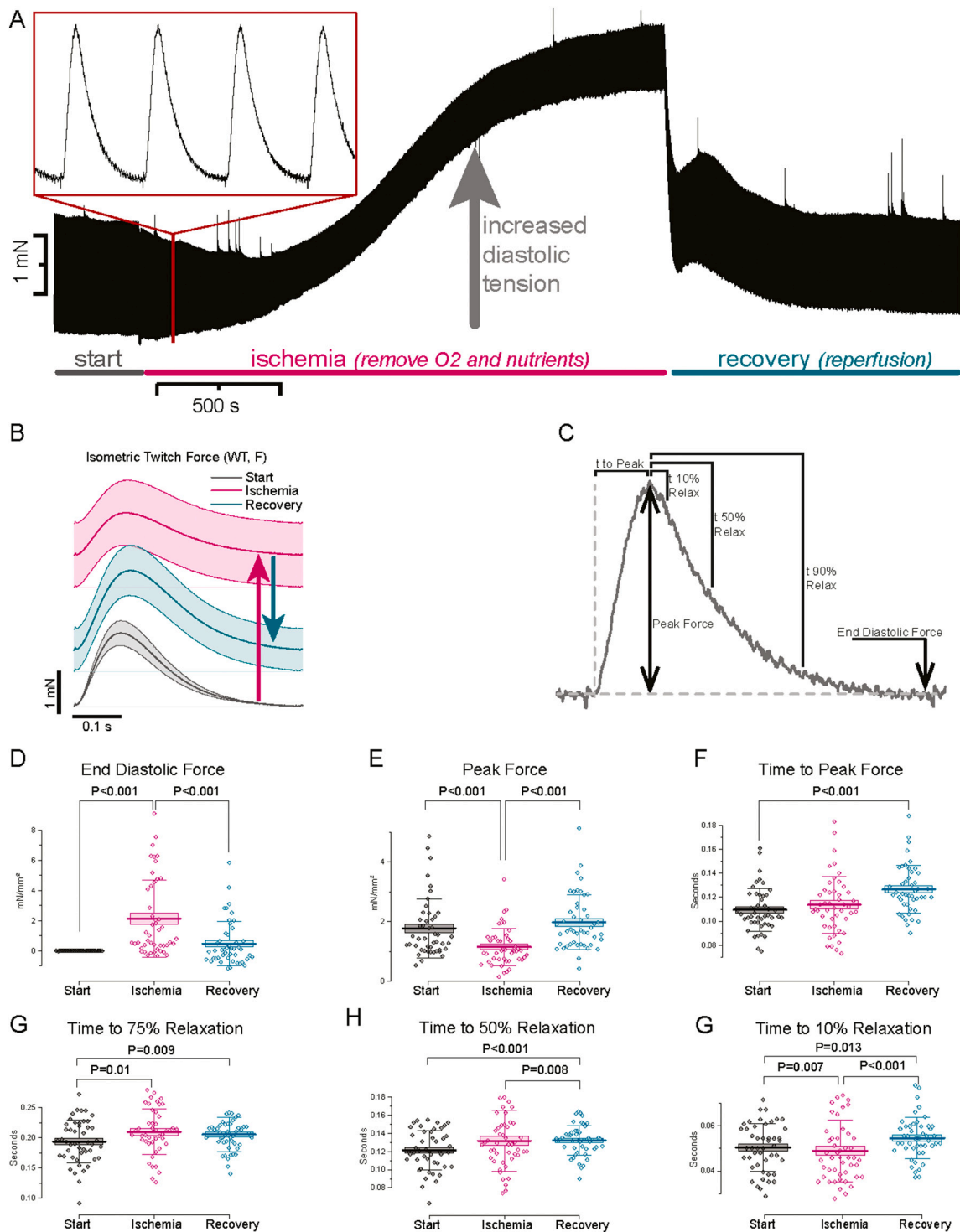


Fig. 1. Living myocardial slices from adult mice demonstrated expected response to ischemic stress. **A)** Each contraction of the slice generated a force transient (inset) which were recorded for the duration of the experiment. **B)** Compiled data for force transients collected over an entire experiment demonstrated an increase in diastolic force and a reduction in contractility during ischemia, and a return toward baseline function during the recovery period. 5–20 transients were averaged and used to calculate the **C)** end diastolic force, peak height, time to peak force, time from peak force to 75 % relaxation, time from peak force to 50 % relaxation, and the time from peak force to 10 % relaxation. **D)** Ischemia increased end-diastolic force. **E)** Ischemia reduced peak force compared with that at the start and after recovery. **F)** Time to peak force increased after Recovery, compared to Start. **G)** Time from Peak force to 75 % relaxation demonstrated late phase diastole is extended after ischemia and recovery. **H)** After recovery, the time from peak force to 50 % relaxation increased, compared with that at the start or after ischemia. **I)** The time from peak force to 10 % relaxation decreased after ischemia and increased after recovery, compared with the start. **D–I)** Start, Ischemia, and Recovery: $N = 26$, $n = 47$; Pairwise comparisons with Sidaks multiple comparisons.

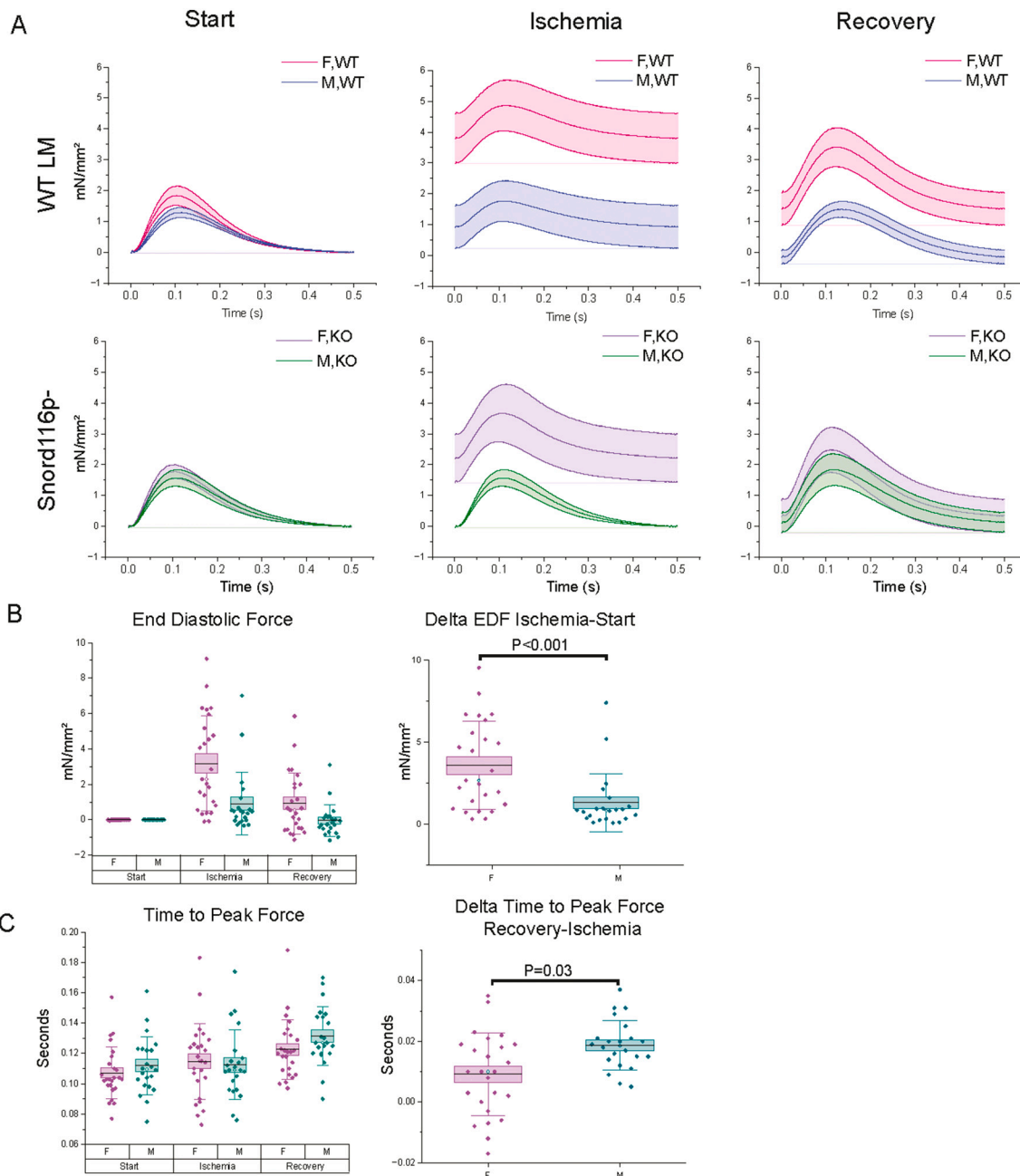


Fig. 2. Slices from female mice experienced a faster and more dramatic response to ischemia. **A)** Averaged force transient data revealed a larger increase in diastolic force during ischemia and recovery when myocardial tissue was derived from females, as compared with tissue from males. **B)** Compared with slices derived from males, slices from female donor hearts experienced a greater increase in end-diastolic force during ischemia. **C)** The difference in time to peak force between Ischemia and Recovery was less in female mice, compared to males. **B** and **C)** Males: $N = 13$, $n = 22$; Females: $N = 13$, $n = 25$; estimate of fixed effects.

LM Female: $N = 7$, $n = 13$; Snord116p- Male: $N = 6$, $n = 11$; Snord116p- Female: $N = 6$, $n = 12$.

3. Results

3.1. Ischemia induces elevated diastolic tension, reduced force, and prolonged kinetics after mild ischemic stress

Using myocardial slices derived from male and female Snord116 paternal knockout (Snord116p-) mice and wildtype littermates (WT LM), we monitored isometric twitches at the start, after 30 min of ischemia, and after 15 min of recovery (Fig. 1A and B). We observed no differences in isometric contractility at the start of the experiment

between genotypes or sexes (Supplemental Fig. 1A). Ischemia is known to induce a rise in diastolic tension, reduce generated force and slow contraction and relaxation kinetics [17]. The rise in diastolic force is caused by the inability of cardiomyocytes to remove calcium. Our early ischemia protocol recapitulated all these effects. This appeared as a rise in end diastolic force (EDF) minutes after exchanging into the hypoxic, hypoglycemic solution (Fig. 1A). Thirty minutes of ischemia increased EDF by 2.04 mN/mm^2 compared to the start ($P < 0.001$; Fig. 1D and Supplemental Tables 1–4). After the 15-min recovery period, EDF returned to the level observed at the start. The generated force (peak force) was reduced by 0.618 mN/mm^2 after ischemia and returned to baseline levels after the recovery period ($P < 0.001$; Fig. 1E, Supplemental Tables 5–7). Ischemic stress caused a delay in contractile and

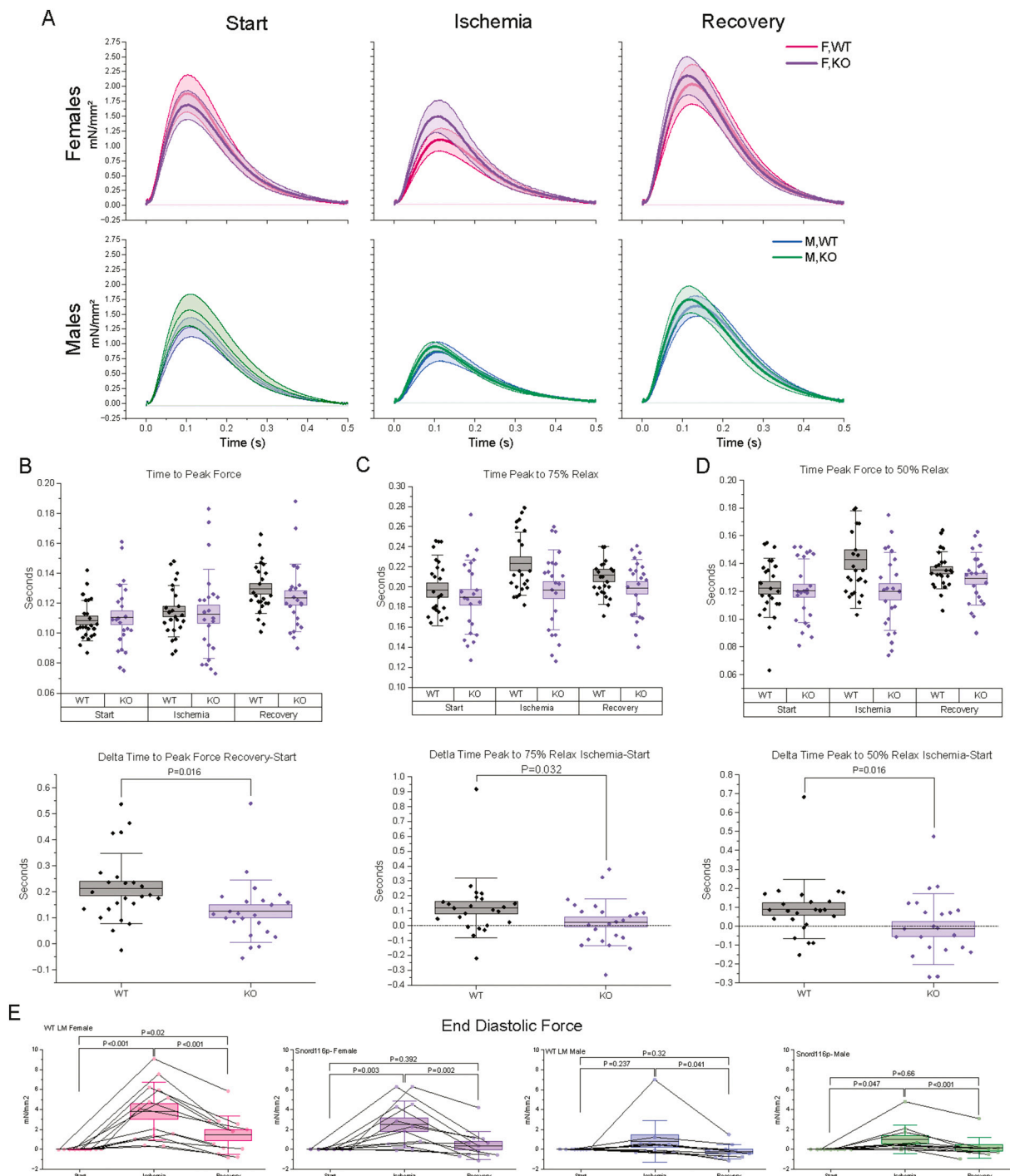


Fig. 3. Snord116 loss impacts cardiomyocyte kinetics during and after ischemic stress. **A)** Averaging of force transients demonstrated that myocardial slices derived from wildtype littermates (WT LM) underwent a more dramatic rightward shift after ischemia and recovery compared with those from Snord116 paternal knockout mice (Snord116p-) in males and females. **B)** The change in requisite time to reach peak force between Start and Recovery was markedly less in Snord116p- slices, compared with that observed for WT LM). Snord116p- slices demonstrated a smaller increase in time from peak force to **C)** 75 % and **D)** 50 % relaxation during ischemia, compared with that for WT LM slices. **B–D)** WT LM: $N = 14$, $n = 24$; Snord116p-: $N = 12$, $n = 23$; estimates of fixed effects. **E)** Loss of Snord116 protected end diastolic force after recovery in tissue derived from females (WT LM Male: $N = 7$, $n = 11$; WT LM Female: $N = 7$, $n = 13$; Snord116p- Male: $N = 6$, $n = 11$; Snord116p- Female: $N = 6$, $n = 12$; Two-sided, paired T -Test).

relaxation kinetics as demonstrated by time to peak force and time from peak to 10 %, 50 % and 75 % relaxation (Fig. 1C). Compared with timing at the start, the time to peak force increased by 0.018 s (s) after recovery, ($P < 0.001$; Fig. 1F, Supplemental Tables 8–11). The observed increase in time to peak force (i.e., delay) confirmed that the ischemic stress applied to each slice in the model extended systole. The time from peak

force to 75 % relaxation (i.e., late relaxation) increased after ischemia and remained elevated after recovery (Start to Ischemia: $P = 0.01$; Start to Recovery $P = 0.009$; Fig. 1G, Supplemental Tables 12–15). The time from peak force to 50 % relaxation increased after the recovery period, compared to the start ($P < 0.001$; Fig. 1H, Supplemental Tables 16–19). The time from peak force to 10 % relaxation (i.e., early relaxation)

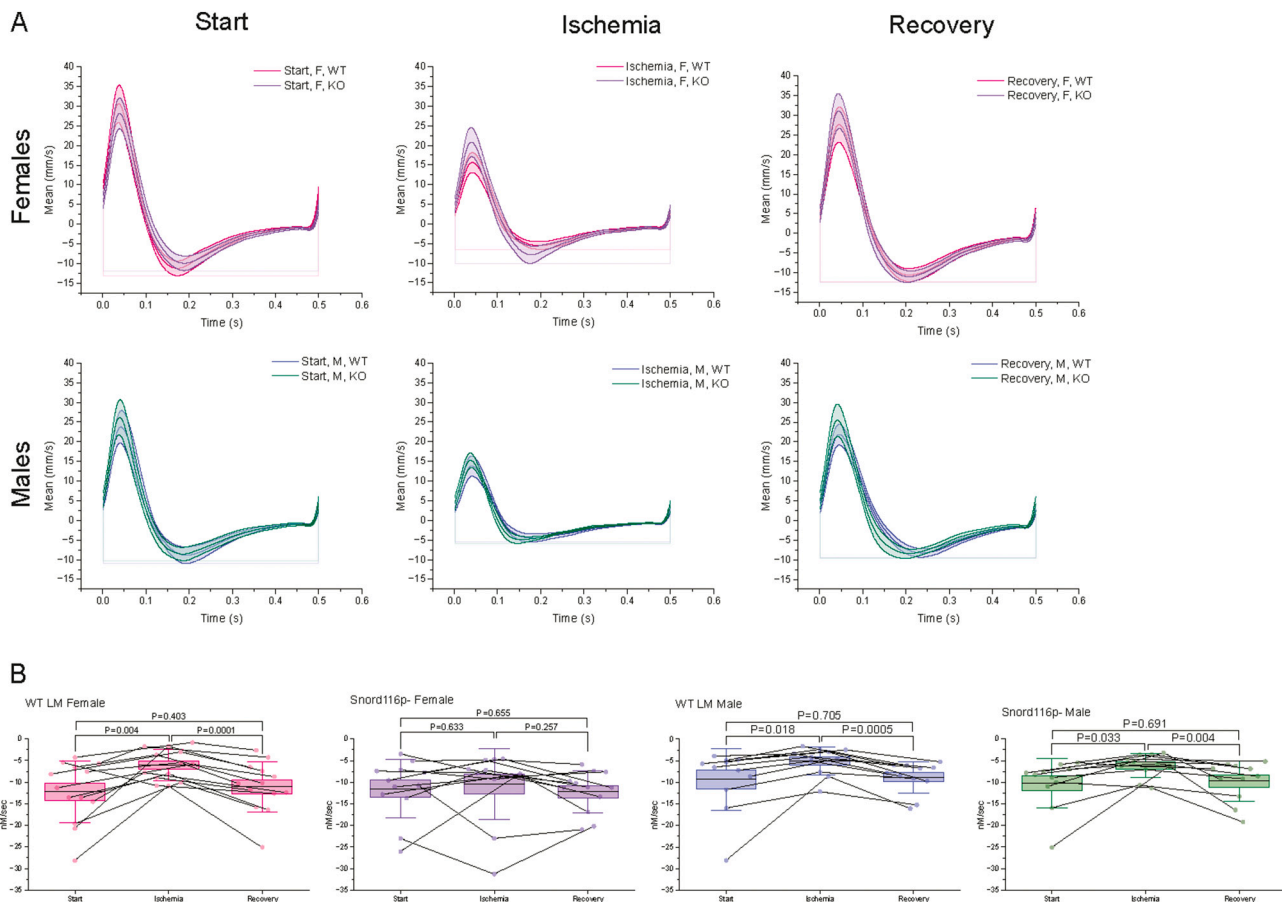


Fig. 4. Loss of Snord116 protected minimum rate of relaxation in female tissue during ischemia. **A)** Plots of the averaged the rate of contraction and relaxation. **B)** Loss of Snord116 protected minimum relaxation rate in females during ischemia (WT LM Male: N = 7, n = 11; WT LM Female: N = 7, n = 13; Snord116p- Male: N = 6, n = 11; Snord116p- Female: N = 6, n = 12; Two-sided, paired T-Test).

decreased after 30 min of ischemia, and then increased after recovery, compared to the start (Start to Ischemia: $P = 0.007$; Start to Recovery $P = 0.013$; Fig. 11, Supplemental Tables 20–23). These data indicated that ischemic stress increased the rate of early relaxation while slowing the rate of late relaxation. Each metric demonstrated the expected response to mild ischemic stress and demonstrated the utility of the slice model to investigate the acute effect(s) of ischemia and reperfusion on cardiomyocyte function.

3.2. Females show a greater ischemia-induced increase in end-diastolic force (EDF) and more rapid changes in contractile kinetics than males

Isometric twitches from males and females were similar at the start of the experiment (Fig. 2A, left panels). Upon exposure to 30 min of ischemia, EDF of female tissue increased by 2.26 mN/mm^2 more than male tissue ($P < 0.001$; Fig. 2A and B, Supplemental Tables 1, 2, and 24). Both male and female slices exhibited impaired contractile kinetics as shown by increased contraction time, with females showing an earlier onset of prolonged contractile time than males. Female slices increased time to peak force during the 30 min of ischemia, and further during the 15-min recovery period. By contrast, time to peak force did not increase in males during ischemia but incurred a larger increase in time to peak force during the recovery period. Time to peak force continued to slow following ischemia during recovery with females showing 9 ms less of a prolongation to peak force compared to males ($P = 0.03$; Fig. 2C, Supplemental Tables 9 and 25). These data suggested that female ventricular tissue is affected more dramatically and quickly than male tissue when experiencing ischemia.

3.3. Snord116 loss protects cardiomyocytes from ischemia-induced prolongation of systole and delays the slowing of relaxation

Isometric twitches are overlaid in Fig. 3 to illustrate the kinetic changes induced by ischemia in WT LM slices, compared with those derived from Snord116p- mice (Fig. 3A, see also Supplemental Fig. 2). The increase in time to peak force between start and recovery was 0.0097 s shorter for slices from Snord116p- mice, compared to those from WT LM ($P = 0.015$; Fig. 3B, Supplemental Table 9 and 26). Although this appeared to be a small change, the WT LM slices underwent a 21.1 % increase in time to peak force, while those from Snord116p- animals only experienced an 11.6 % increase, suggesting that the loss of Snord116 was protective. Snord116p- animals were also protected from changes in diastolic function as evident from a reduced prolongation in time from peak force to 75 % and 50 % relaxation experienced during ischemia of 0.015 s and 0.011 s, respectively (Time peak to 75 % relax: $P = 0.032$; Time peak to 50 % Relax: $P = 0.016$; Fig. 3C and D, Supplemental Tables 13 and 17). During the recovery period, the time from peak to 75 % and 50 % relaxation increased in slices derived from Snord116p- mice to match the delay experienced by WT LM slices (Supplemental Tables 27 and 28). Although we did not find a significant effect of genotype on EDF by linear mixed model, by evaluating how EDF changed in each group over the course of the experiment, we found a protective effect of Snord116p- in female tissue. As described above, female tissue underwent a more significant increase in EDF during ischemia, compared with males, so differences between WT LM and Snord116p- tissue were more obvious when separating tissue by sex. The female WT LM slice had increased EDF after the recovery period, compared with the start ($P = 0.02$; Fig. 3E), while female

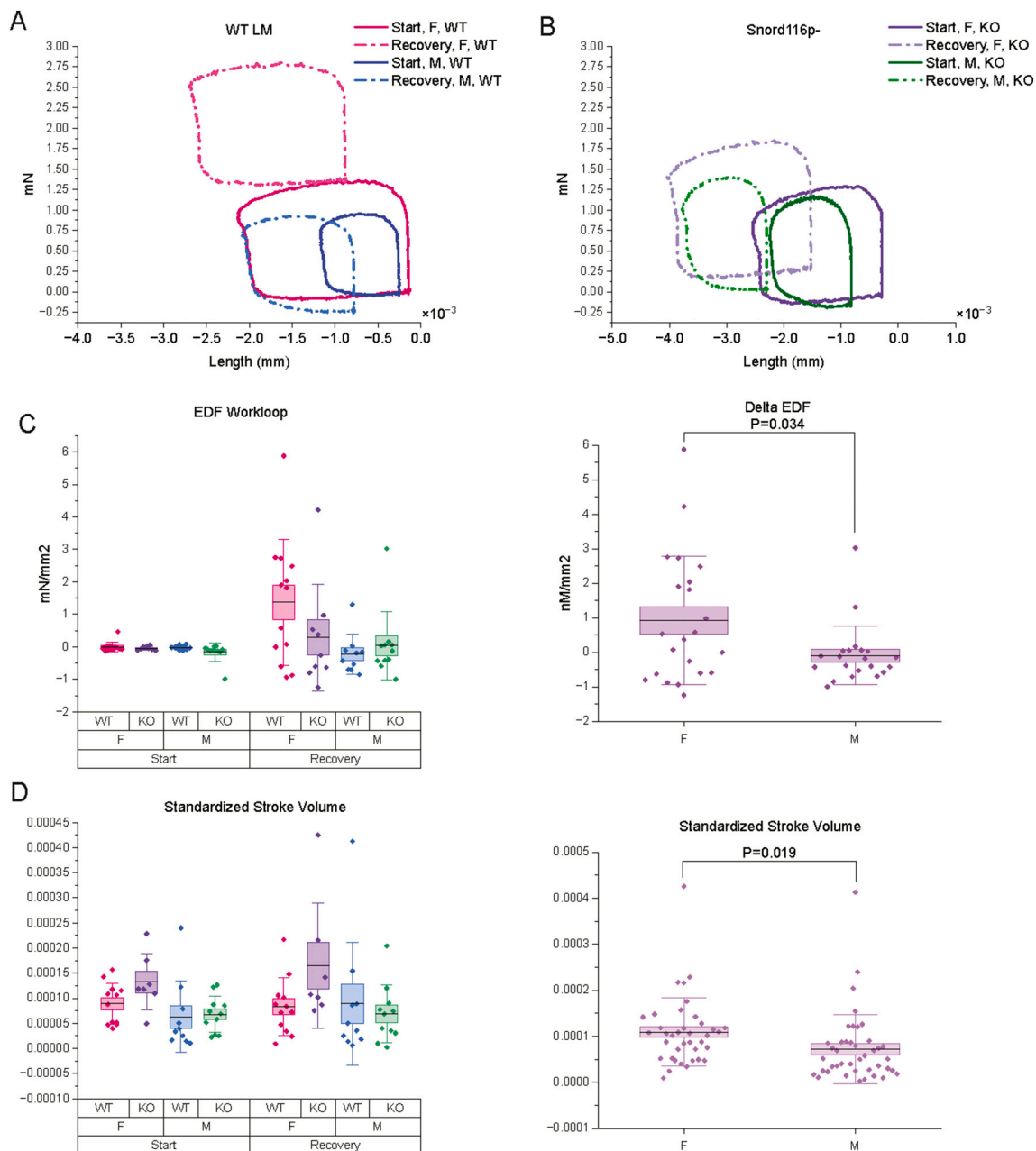


Fig. 5. Work-loops support amplified end diastolic force in female slices after ischemia, compared with males. Work-loops from A) WT LM and B) Snord116p- slice at start and after recovery. C) Tissue derived from females incurs a larger increase in EDF, compared with that from males. D) Slices derived from females demonstrated increased stroke volume by work-loop, compared with males. C–D) Pairwise comparisons with Sidak's multiple comparisons (Males: N = 12, n = 21; Females: N = 10, n = 21).

Snord116p- slices returned to baseline levels ($P = 0.392$; Fig. 3E). These data demonstrated that loss of Snord116 protected cardiomyocytes from slowing of contraction and delayed the reduction in diastolic function caused by ischemic stress. Additionally, loss of Snord116 protected female tissue from increased diastolic tension after the recovery period.

3.4. Loss of Snord116 protects female myocardium from ischemia-induced reduction in diastolic performance

The change in force over time demonstrated that ischemia reduced the maximum rate of force generation ($+df/dt$) and increased the minimum rate of force relaxation ($-df/dt$) in each sex and genotype, reaffirming that this mild ischemia protocol slows the rate of contraction and relaxation (Supplemental Fig. 3). The minimum $-df/dt$ increased

during ischemia in WT LM female slices ($P = 0.004$) but was protected in the female Snord116p- slices ($P = 0.633$; Fig. 4). The loss of Snord116 expression enabled the preservation of relaxation rates under ischemic stress in female tissue.

3.5. Ischemia increases EDF in working female slices more than male slices

To assess the effect of Snord116 expression and sex on myocardial functional decline following an ischemic insult, we subjected myocardial slices to a force feedback system to generate work-loops at the start of the experiment and after the recovery period. The female tissue exhibited a 0.998 mN/mm^2 larger increase in EDF between start and after recovery, compared with tissue from males ($P = 0.032$; Fig. 5A-C,

see also Supplemental Fig. 5). Additionally, the work-loop analysis demonstrated that tissue derived from female donors generated a larger stroke length compared to tissue from male donors ($P = 0.019$; Fig. 5D and Supplemental Table 29). These findings underscore the strength of the myocardial slice model to evaluate sex-based differences in cardiomyocyte function under physiological and pathological conditions.

4. Discussion

We developed a model using living myocardial slices to determine the myocardial response during the onset of and after mild ischemic stress. After 30 min of simulated ischemia, myocardial slices exhibited increased end diastolic force (EDF), reduced twitch force, and diastolic performance. After 15 min of recovery (i.e., reperfusion), slices exhibited a normalization of EDF and peak height to levels observed prior to ischemia, while the kinetics of systole and diastole were prolonged. Ischemia induced a greater increase in EDF in female slices than males which held in both wild type littermates (WT LM) and Snord116 paternal knockout (Snord116p-) mice. Males took longer than females to exhibit slowed systolic kinetics. For both males and females, we found that myocardial slices from Snord116p- mice were less sensitive to ischemia-dependent modification of contractile and relaxation kinetics, as compared with slices from WT LM. Our results are consistent with Hayman et al. (2023) who described a model of ischemia/reperfusion injury in which living myocardial slices were cultured under hypoxic conditions and generated reduced active force after 19–24 h in culture [19]. Here, we determined that real-time changes in cardiomyocyte kinetics, generated force, and EDF are detectable after only 30 min of ischemia and persist directly after ischemic stress in mouse myocardial slices.

Our data revealed that relative to male myocardial slices, female slices exposed to ischemic stress experienced a more dramatic increase in end-diastolic force and more quickly slowed contractile kinetics. These data align with observations from Bell et al. (2016), who demonstrated that upon ischemic stress, isolated female rat myocytes experienced a greater increase in diastolic calcium level and calcium amplitude, compared with normal male myocytes [20]. It is well documented that pre-menopausal female rodents exhibit increased tolerance to ischemia and reduced infarct size after MI, compared with males, and that estrogen plays a cardio-protective role [21–23]. However, estrogen replacement therapy was shown to increase cardiovascular risk in post-menopausal women [24]. Thus, our data and those of others suggest that sex is likely an important factor in ischemia and warrants deeper investigation to understanding the apparent differences in susceptibility to ischemia. The myocardial slice model with ischemia-reperfusion described here has exciting potential to help identify factors and mechanisms underlying sex-based differences in patient risk and outcomes for cardiovascular disease.

We found that loss of Snord116 expression was beneficial to cardiomyocyte function during ischemia and after reperfusion. This result was surprising as the loss of Snord116 (PWS) leads to an increased risk of cardiovascular disease. We hypothesize that long term changes to DNA methylation in PWS patients leads to metabolic disorder and CVD, while these same shifts at certain timepoints may lead to improved resistance to ischemia as observed in this experiment. We performed our experiments during normal working hours, corresponding to the light phase of the mouse day and Zeitgeber Time 6 (ZT6). For the cerebral cortex, ZT6 was the peak time for differential methylation between Snord116p- mice and WT LM [25]. Accordingly, it would be useful to replicate our myocardial slice experiments at ZT18, during dark hours, to determine whether the phenotype generated by Snord116 loss is affected. One of the genes Coulson et al. (2018) identified as differentially methylated in Snord116p- mice, and also in PWS patients, codes for NBCe1, a $\text{Na}^+/\text{HCO}_3^-$ cotransporter expressed on the sarcolemma of cardiomyocytes, and regulates pH by transporting HCO_3^- [25,26]. Cardiomyocyte-specific deletion of NBCe1 did not produce changes to contraction or

relaxation at baseline, but was found to reduce cardiomyocyte apoptosis after ischemia/reperfusion injury in vivo [27,28]. Thus, determination of myocardial NBCe1 levels and whether changes in NBCe1 expression or alternative splicing contribute to the phenotype of Snord116p-derived slices is of interest. Furthermore, investigating whether rates of cardiomyocyte apoptosis following MI are decreased in hearts of Snord116p- mice relative to those in WT LM hearts may help to better understand the degree of protection conferred by Snord116 loss and could be conducted in our experimental system with a longer duration of ischemia. Although more research is required to define how Snord116 acts mechanistically, our research supports Snord116 as a target for therapeutic intervention for the treatment of ischemic cardiac injury.

Supplementary data to this article can be found online at <https://doi.org/10.1016/j.jmccpl.2025.100291>.

CRediT authorship contribution statement

Lucy E. Pilcher: Writing – review & editing, Writing – original draft, Methodology, Investigation, Data curation, Conceptualization. **Emma-leigh Hancock:** Methodology, Investigation, Formal analysis, Data curation. **Akshay Neeli:** Methodology, Investigation, Formal analysis, Data curation. **Maria Skolnick:** Software, Methodology, Formal analysis, Data curation. **Matthew A. Caporizzo:** Writing – review & editing, Writing – original draft, Validation, Software, Methodology, Formal analysis, Data curation. **Bradley M. Palmer:** Writing – review & editing, Writing – original draft, Methodology, Investigation, Formal analysis, Data curation. **Jeffrey L. Spees:** Writing – review & editing, Writing – original draft, Visualization, Validation, Supervision, Resources, Project administration, Methodology, Investigation, Funding acquisition, Formal analysis, Data curation, Conceptualization.

Author contributions

LP, MC, BP, and JS designed the experiments. LP, EH, AN, MS, MC and JS performed the experiments, assays and data analysis. LP, MC and JS wrote the paper.

Declaration of Generative AI and AI-assisted technologies in the writing process

The authors did not use generative AI or AI-assisted technologies in the development of this manuscript.

Declaration of competing interest

Dr. Spees holds several patents in the areas of regenerative medicine, human epicardial progenitor cell biology, and secreted growth factors. He is co-founder and Chief Scientific Officer of Samba BioLogics, Inc. Dr. Palmer is an employee of IonOptix.

Acknowledgements

The Snord116p- mouse strain was generously provided by Dr. Rudolph L. Leibel, Columbia University. This work was supported, in part, by National Institutes of Health (NIH) grant HL132264 (to JLS). Additional support was provided by the Cardiovascular Research Institute of Vermont (CVRI-VT).

References

- [1] Ahmad FB, Anderson RN. The leading causes of death in the US for 2020. *Jama* 2021;325(18):1829–30.
- [2] Murphy E, Steenbergen C. Ion transport and energetics during cell death and protection. *Physiology (Bethesda)* 2008;23:115–23.
- [3] Buja LM, Vela D. Cardiomyocyte death and renewal in the normal and diseased heart. *Cardiovasc Pathol* 2008;17(6):349–74.

- [4] Goldspink DF, Burniston JG, Tan L-B. Cardiomyocyte death and the ageing and failing heart. *Exp Physiol* 2003;88(3):447–58.
- [5] Lerner DJ, Kannel WB. Patterns of coronary heart disease morbidity and mortality in the sexes: a 26-year follow-up of the Framingham population. *Am Heart J* 1986; 111(2):383–90.
- [6] Bugiardini R, Cenko E. Sex differences in myocardial infarction deaths. *Lancet* 2020;396(10244):72–3.
- [7] Valero-Masa MJ, et al. Sex differences in acute myocardial infarction: is it only the age? *Int J Cardiol* 2017;231:36–41.
- [8] Abbas N, Perbellini F, Thum T. Non-coding RNAs: emerging players in cardiomyocyte proliferation and cardiac regeneration. *Basic Res Cardiol* 2020;115: 1–20.
- [9] Yuan T, Krishnan J. Non-coding RNAs in cardiac regeneration. *Front Physiol* 2021; 12:650566.
- [10] Powell WT, et al. A Prader-Willi locus lncRNA cloud modulates diurnal genes and energy expenditure. *Hum Mol Genet* 2013;22(21):4318–28.
- [11] Bertone G, Bilo G. Cardiovascular features of Prader-Willi syndrome. *J Hypertens* 2021;39:e335.
- [12] Bieth E, et al. Highly restricted deletion of the SNORD116 region is implicated in Prader-Willi syndrome. *Eur J Hum Genet* 2015;23(2):252–5.
- [13] Pace M, et al. Loss of Snord116 impacts lateral hypothalamus, sleep, and food-related behaviors. *JCI Insight* Jun 18 2020;5(12).
- [14] Pilcher L, Solomon L, Dragon JA, Gupta D, Spees JL. The neural progenitor cell-associated transcription factor FoxG1 regulates cardiac Epicardial cell proliferation. *Stem Cells Int* 2024;2024.
- [15] Coulson RL, Powell WT, Yasui DH, Dileep G, Resnick J, LaSalle JM. Prader-Willi locus Snord116 RNA processing requires an active endogenous allele and neuron-specific splicing by Rbfox3/NeuN. *Hum Mol Genet* 2018;27(23):4051–60.
- [16] Sonnenblick E, Kirk E. Effects of hypoxia and ischemia on myocardial contraction: alterations in the time course of force and ischemia-dependent inhomogeneity of contractility. *Cardiology* 1971;56(1–6):302–13.
- [17] Varma N, Morgan JP, Apstein CS. Mechanisms underlying ischemic diastolic dysfunction: relation between rigor, calcium homeostasis, and relaxation rate. *Am J Phys Heart Circ Phys* 2003;284(3):H758–71.
- [18] Ding F, et al. SnoRNA Snord116 (Pwcr1/MBII-85) deletion causes growth deficiency and hyperphagia in mice. *PLoS One* 2008;3(3):e1709.
- [19] Hayman D, Terracciano CM. Development of an ischemia/reperfusion injury model in the living myocardial slice. *Biophys J* 2023;122(3):165a.
- [20] Bell JR, Curl CL, Harding TW, Vila Petroff M, Harrap SB, Delbridge LM. Male and female hypertrophic rat cardiac myocyte functional responses to ischemic stress and β -adrenergic challenge are different. *Biol Sex Differ* 2016;7:1–15.
- [21] Ostadal B, et al. Developmental and sex differences in cardiac tolerance to ischemia–reperfusion injury: the role of mitochondria. *Can J Physiol Pharmacol* 2019;97(9):808–14.
- [22] Bouma W, et al. Sex-related resistance to myocardial ischemia-reperfusion injury is associated with high constitutive ARC expression. *Am J Phys Heart Circ Phys* 2010; 298(5):H1510–7.
- [23] Ross JL, Howlett SE. Age and ovariectomy abolish beneficial effects of female sex on rat ventricular myocytes exposed to simulated ischemia and reperfusion. *PLoS One* 2012;7(6):e38425.
- [24] Rossouw JE, et al. Risks and benefits of estrogen plus progestin in healthy postmenopausal women: principal results from the Women's Health Initiative randomized controlled trial. *Jama* 2002;288(3):321–33.
- [25] Coulson RL, et al. Snord116-dependent diurnal rhythm of DNA methylation in mouse cortex. *Nat Commun* 2018;9(1):1616.
- [26] Wang H-S, Chen Y, Vairamani K, Shull GE. Critical role of bicarbonate and bicarbonate transporters in cardiac function. *World J Biol Chem* 2014;5(3):334.
- [27] Vairamani K, et al. NBCe1 Na⁺-HCO₃-cotransporter ablation causes reduced apoptosis following cardiac ischemia-reperfusion injury in vivo. *World J Cardiol* 2018;10(9):97.
- [28] Lu M, et al. The electrogenic sodium bicarbonate cotransporter and its roles in the myocardial ischemia-reperfusion induced cardiac diseases. *Life Sci* 2021;270: 119153.